EXTENDED PDF FORMAT
SPONSORED BY
More Differentiation. With Less Variation.
Reduce Variation in Your Stem Cell Experiments.
R&D SYSTEMS
www.rndsystems.com

# Photomechanical Responses in *Drosophila* Photoreceptors

Roger C. Hardie and Kristian Franze

*Science* **338**, 260 (2012);
DOI: 10.1126/science.1222376

*This copy is for your personal, non-commercial use only.*

**If you wish to distribute this article to others**, you can order high-quality copies for your colleagues, clients, or customers by clicking here.

**Permission to republish or repurpose articles or portions of articles** can be obtained by following the guidelines here.

***The following resources related to this article are available online at www.sciencemag.org (this information is current as of March 3, 2013 ):***

**Updated information and services,** including high-resolution figures, can be found in the online version of this article at:
http://www.sciencemag.org/content/338/6104/260.full.html

**Supporting Online Material** can be found at:
http://www.sciencemag.org/content/suppl/2012/10/10/338.6104.260.DC1.html

A list of selected additional articles on the Science Web sites **related to this article** can be found at:
http://www.sciencemag.org/content/338/6104/260.full.html#related

This article **cites 30 articles**, 9 of which can be accessed free:
http://www.sciencemag.org/content/338/6104/260.full.html#ref-list-1

This article has been **cited by** 3 articles hosted by HighWire Press; see:
http://www.sciencemag.org/content/338/6104/260.full.html#related-urls

This article appears in the following **subject collections:**
Cell Biology
http://www.sciencemag.org/cgi/collection/cell_biol

Downloaded from www.sciencemag.org on March 3, 2013

*Science* (print ISSN 0036-8075; online ISSN 1095-9203) is published weekly, except the last week in December, by the American Association for the Advancement of Science, 1200 New York Avenue NW, Washington, DC 20005. Copyright 2012 by the American Association for the Advancement of Science; all rights reserved. The title *Science* is a registered trademark of AAAS.

friction is present, total force on the EVL also has a geometry-independent contribution, where retrograde flow of actin and myosin-2 is resisted by friction (termed "flow-friction motor"; Fig. 3A). In the embryo, friction will arise when the flow velocity in the ring is different from the velocity of the adjacent material, such as the yolk cell plasma membrane and the yolk cytoplasm. Consistent with this, we observed differential flow velocities between the actomyosin in the ring and adjacent microtubules within the YSL (fig. S6). This flow-friction motor pulls the EVL in a direction opposite to the actomyosin flow, operates at any stage, and can drive epiboly before passing the equator (Fig. 3A and fig. S11). Notably, friction-resisted flow provides additional tension in the AV direction, consistent with the small degree of tension anisotropy observed in the laser ablation experiments (Fig. 2B). Furthermore, experimentally measured flow profiles within the EVL and the actomyosin ring, as well as the relative tensions obtained from laser ablation, are accurately predicted by our theoretical description at all stages when friction against the substrate is taken into account (Fig. 3B). To conclude, we identified two distinct modes of ring propulsion: a cable-constriction motor due to circumferential contraction of the YSL actomyosin network, and a flow-friction motor due to contraction along the AV axis of the network.

We next asked if the flow-friction motor is sufficient to drive EVL epiboly. To this end, we took advantage of the predicted geometry dependence of the cable-constriction motor. Because the cable-constriction motor cannot exert a net force on the EVL when positioned right at the equator, propulsion by this motor would be hindered when the yolk cell is deformed from its original spherical geometry into a cylindrical shape. We thus deformed the yolk cell into a cylindrical shape by aspirating pre–gastrula-stage embryos (2.5 hpf ) into agarose tubes of a diameter smaller than that of the embryo and analyzed resulting changes in EVL movements. To verify that the actomyosin ring is unperturbed in cylindrical embryos, we analyzed the distribution and flow of actin and myosin-2 within the YSL of cylindrical embryos. We found that both the accumulation of actin and myosin-2 in a ring-like structure adjacent to the EVL/YSL border and their retrograde flows from the vegetal pole toward the EVL/YSL border were largely unaffected in cylindrical embryos as compared to normal-shaped control embryos (Fig. 4 and movie S10). This suggests that the actomyosin ring remains intact in cylindrical embryos. We observed that EVL movements were largely unaffected in cylindrical embryos and proceeded with velocities similar to those of spherical control embryos ($2.0 \pm 0.2$ μm/min compared to $1.9 \pm 0.1$ μm/min at 60 to 70% epiboly; compare Figs. 4D and 2D). This shows that the cable-constriction motor is not essential for EVL epiboly movements and indicates that the flow-friction motor is sufficient to drive this process.

Our findings have major implications for the function of actomyosin rings in morphogenesis. Whereas the prevalent model of actomyosin ring function assumes circumferential contraction as the main force-generating process, we present evidence that friction-resisted actomyosin flows can represent an equally important process mediating ring function. This raises the possibility of a more general role of cortical flows in morphogenetic pattern formation processes (*18*).

### References and Notes


1. S. E. Lepage, A. E. E. Bruce, *Int. J. Dev. Biol.* **54**, 1213 (2010).
2. D. A. Kane *et al.*, *Development* **123**, 47 (1996).
3. M. Siddiqui, H. Sheikh, C. Tran, A. E. E. Bruce, *Dev. Dyn.* **239**, 715 (2010).
4. M. Köppen, B. G. Fernández, L. Carvalho, A. Jacinto, C.-P. Heisenberg, *Development* **133**, 2671 (2006).
5. F. A. Barr, U. Gruneberg, *Cell* **131**, 847 (2007).
6. J. M. Sawyer *et al.*, *Dev. Biol.* **341**, 5 (2010).
7. A. Jacinto, S. Woolner, P. Martin, *Dev. Cell* **3**, 9 (2002).
8. M. S. Hutson *et al.*, *Science* **300**, 145 (2003).
9. P. Martin, J. Lewis, *Nature* **360**, 179 (1992).
10. J. C. Cheng, A. L. Miller, S. E. Webb, *Dev. Dyn.* **231**, 313 (2004).
11. B. A. Holloway *et al.*, *PLoS Genet.* **5**, e1000413 (2009).
12. M. Mayer, M. Depken, J. S. Bois, F. Jülicher, S. W. Grill, *Nature* **467**, 617 (2010).
13. K. Kruse, J. F. Joanny, F. Jülicher, J. Prost, K. Sekimoto, *Eur. Phys. J. E* **16**, 5 (2005).
14. G. Salbreux, J. Prost, J. F. Joanny, *Phys. Rev. Lett.* **103**, 058102 (2009).
15. D. Bray, J. G. White, *Science* **239**, 883 (1988).
16. L. P. Cramer, *Front. Biosci.* **2**, d260 (1997).
17. J. Howard, *Mechanics of Motor Proteins and Cytoskeleton* (Sinauer Associates, Sunderland, MA, 2001).
18. N. W. Goehring *et al.*, *Science* **334**, 1137 (2011).



**Acknowledgments:** We are grateful to M. Sixt, T. Bollenbach, and E. Martin-Blanco for advice and the service facilities of the IST Austria and MPI-CBG for continuous help. M.B., G.S., S.W.G., and C.-P.H. synergistically and equally developed the presented ideas and the experimental and theoretical approaches. M.B. and P.C. performed the experiments; G.S. developed the theory; and R.H., F.O., and J.R. contributed to the experimental work. This work was supported by a grant from the Fonds zur Förderung der wissenschaftlichen Forschung (FWF) and the Deutsche Forschungsgemeinschaft (DFG) (I930-B20) to C.-P.H., S.W.G., and G.S.


### Supplementary Materials

www.sciencemag.org/cgi/content/full/338/6104/257/DC1
Supplementary Text
Figs. S1 to S16
Materials and Methods
References (*19*–*36*)
Movies S1 to S10


1 May 2012; accepted 10 September 2012
10.1126/science.1224143


# Photomechanical Responses in *Drosophila* Photoreceptors


**Roger C. Hardie* and Kristian Franze**



**Phototransduction in *Drosophila* microvillar photoreceptor cells is mediated by a G protein–activated phospholipase C (PLC). PLC hydrolyzes the minor membrane lipid phosphatidylinositol 4,5-bisphosphate ($PIP_2$), leading by an unknown mechanism to activation of the prototypical transient receptor potential (TRP) and TRP-like (TRPL) channels. We found that light exposure evoked rapid PLC-mediated contractions of the photoreceptor cells and modulated the activity of mechanosensitive channels introduced into photoreceptor cells. Furthermore, photoreceptor light responses were facilitated by membrane stretch and were inhibited by amphipaths, which alter lipid bilayer properties. These results indicate that, by cleaving $PIP_2$, PLC generates rapid physical changes in the lipid bilayer that lead to contractions of the microvilli, and suggest that the resultant mechanical forces contribute to gating the light-sensitive channels.**


In most invertebrate photoreceptor cells, the visual pigment (rhodopsin) and other components of the phototransduction cascade are localized within tightly packed microvilli (tubular membranous protrusions), together forming a light-guiding rod-like stack (rhabdomere; Fig. 1). After photoisomerization, rhodopsin activates a heterotrimeric guanine nucleotide–binding protein (Gq protein), releasing its guanosine triphosphate–bound α subunit, which in turn activates phospholipase C (PLC; Fig. 1C). How PLC activity leads to gating of the light-sensitive transient receptor potential channels (TRP and TRPL) in the microvilli is unresolved (*1*–*3*). PLC hydrolyzes the minor membrane phospholipid phosphatidylinositol 4,5-bisphosphate ($PIP_2$), yielding soluble inositol 1,4,5-trisphosphate ($InsP_3$), diacylglycerol (DAG, which remains in the inner leaflet of the microvillar lipid bilayer), and a proton. The light-sensitive channels in *Drosophila* photoreceptors can be activated by a combination of $PIP_2$ depletion and protons (*4*), but it remains unclear how $PIP_2$ depletion might contribute to channel gating. It has been speculated that changes in membrane properties play a role (*4*, *5*), and members of the TRP ion channel family have been repeatedly, although controversially, implicated as mechanosensitive channels (*6*, *7*). This led us to ask whether cleavage of the bulky, charged inositol head group of $PIP_2$ (Fig. 1C) from the inner leaflet might alter the physical properties of the lipid bilayer in the microvilli, resulting in mechanical forces that contribute to channel gating.

Remarkably, *Drosophila* photoreceptors responded to light flashes with small (<1 μm) but rapid contractions that were directly visible in


Department of Physiology, Development and Neuroscience, University of Cambridge, Cambridge CB2 3EG, UK.

*To whom correspondence should be addressed. E-mail: rch14@cam.ac.uk


Downloaded from www.sciencemag.org on March 3, 2013

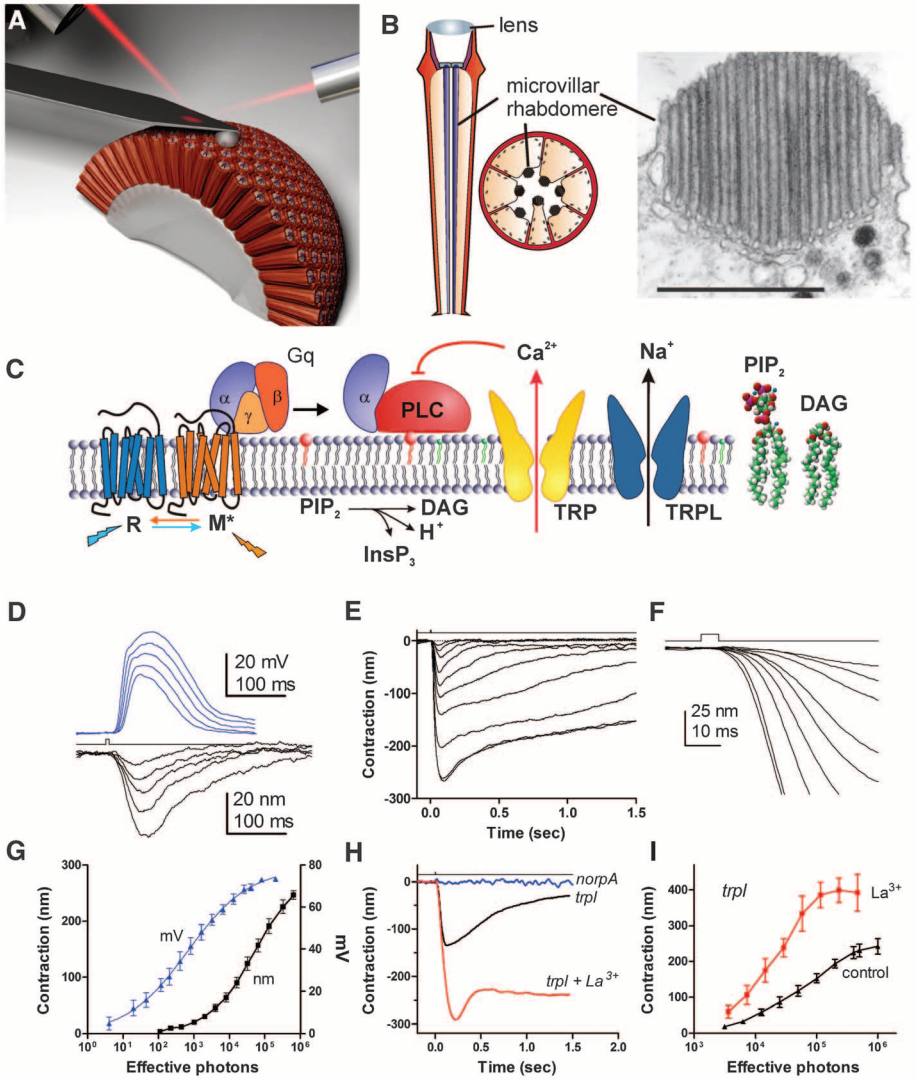


**Fig. 1.** AFM measurements of photomechanical responses. (**A**) An AFM cantilever contacts distal tips of ommatidia in an excised *Drosophila* retina. (**B**) An ommatidium, containing photoreceptors (orange) and pigment cells (red). Elements of the phototransduction cascade are contained within microvillar rhabdomeres (two shown in longitudinal section, seven in cross section), which are rodlike stacks ~80 μm in length containing ~30,000 microvilli. Right: Electron micrograph cross section of a rhabdomere (scale bar, 1 μm), showing tubular microvilli, each ~50 nm in diameter, with lumen in diffusional continuity with the cell body. (**C**) Phototransduction cascade. Rhodopsin (R) is photoisomerized to metarhodopsin (M*), which catalyzes release of the Gq protein α subunit to activate PLC. PLC hydrolyzes $PIP_2$ (red), leaving DAG (green) in the membrane. $Ca^{2+}$ influx via TRP channels inhibits PLC. (**D**) Lower traces: AFM measurements of contractions (cantilever *z*-position) in a wild-type retina in response to 5-ms flashes, with intensity increased from ~200 to 8000 effectively absorbed photons per photoreceptor. Blue traces: Whole-cell current-clamped voltage responses to the same stimuli recorded from a dissociated photoreceptor cell. (**E**) Contractions evoked by 5-ms flashes covering the full intensity range (~200 to $10^6$ photons) in a wild-type retina. (**F**) Same on faster time base. (**G**) Response versus intensity (*R/I*) functions of contractions (nm) from wild-type retinae (mean ± SEM, $N = 13$), and peak voltage (mV) recorded from dissociated photoreceptors (blue; means ± SEM, $N = 6$). (**H**) Responses to flashes (~$5 \times 10^4$ photons) in *trpl* mutant before and after (red) channel block by 50 μM $La^{3+}$ and 10 μM ruthenium red (RR), which prevents inhibition of PLC by $Ca^{2+}$ influx. Blue trace: Lack of response in $norpA^{P24}$ (PLC mutant) despite using flashes of higher intensity (~$2 \times 10^5$ photons; $N = 3$). (**I**) *R/I* function of contractions from *trpl* retinae before and after (red) channel block by $La^{3+}$ and RR (means ± SEM, $N = 5$). For intensity calibration, see fig. S2.

Downloaded from www.sciencemag.org on March 3, 2013

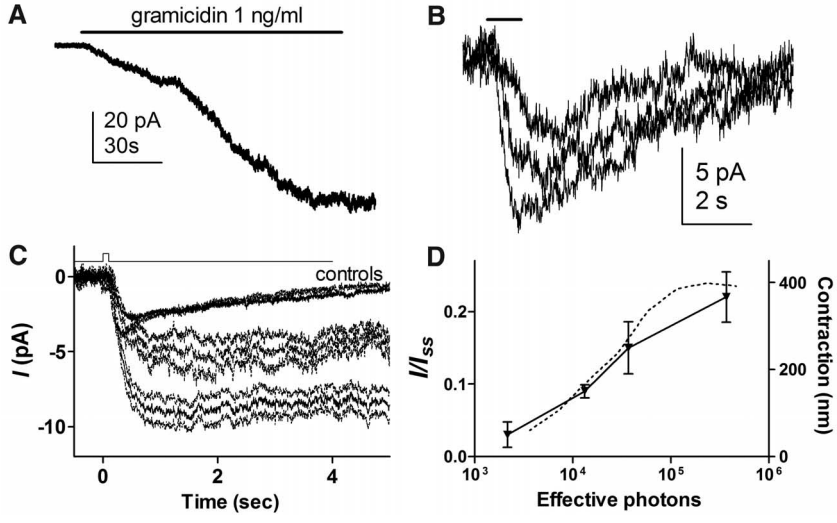


**Fig. 2.** Light-induced modulation of gramicidin channels. (**A**) Whole-cell recordings from *trpl;trp* mutant photoreceptor cell lacking all native light-sensitive channels. Perfusion with gramicidin induced a constitutive inward current. (**B**) Flashes of increasing intensity ($5 \times 10^3$ to $4 \times 10^5$ effective photons), each 1 s (denoted by bar at upper left), up-regulated the current. (**C**) Averaged responses (±SEM) to 100-ms flashes containing $1.3 \times 10^4$ (middle trace, $N = 4$) and $3.7 \times 10^4$ (lower trace, $N = 10$) effective photons (data pooled from *trpl;trp* and *trpl* mutants recorded in the presence of $La^{3+}$ and RR). The same flashes delivered before gramicidin application (controls) induced residual, noise-free transient currents of uncertain origin. (**D**) *R/I* function (after subtracting control responses measured before gramicidin perfusion) expressed as a fraction of the steady-state gramicidin current $I/I_{SS}$ (means ± SEM, $N = 4$). Dotted curve: *R/I* function of contractions measured by AFM in *trpl* mutant in the presence of $La^{3+}$ and RR, replotted from Fig. 1I.

dissociated cells via bright-field microscopy (see movie S1). To obtain improved temporal and spatial resolution, we recorded these photomechanical responses with an atomic force microscope (AFM) (*8*), positioning the AFM cantilever on the distal tips of photoreceptors in a whole excised retina glued to a coverslip (Fig. 1A). Contact force (~100 pN) was maintained constant, so that changes in sample height resulted in immediate, matching changes in the cantilever's *z*-position. Contractions were elicited indefinitely by repeated brief flashes of modest intensity, with kinetics similar to those of electrical responses recorded from dissociated photoreceptors (Fig. 1D and fig. S1). The latencies of contractions induced by the brightest stimuli (4.9 ± 0.9 ms, mean ± SEM, $N$ = 11; Fig. 1F) were significantly shorter than the latencies of voltage responses to the same stimuli (6.6 ± 0.6 ms, $N$ = 6; $P$ = 0.002, unpaired two-tailed $t$ test). Only a few hundred effectively absorbed photons per photoreceptor were required to elicit detectable contractions, which saturated with flashes containing ~$10^6$ photons, corresponding to ~30 effectively absorbed photons per microvillus (Fig. 1, E and G). This intensity dependence overlapped with that of the electrical response (Fig. 1G and supplementary text). Like the electrical responses, the contractions were eliminated in mutants lacking PLC (*norpA*$^{P24}$), which shows that they too required PLC activity (Fig. 1H).

Because PLC activity is normally terminated by $Ca^{2+}$ influx through the light-sensitive channels, net $PIP_2$ hydrolysis is enhanced when the light-sensitive current is blocked (*9*, *10*). We therefore measured contractions in *trpl* mutants expressing only TRP light-sensitive channels before and after blocking TRP channel activity with $La^{3+}$ and ruthenium red (RR). Indeed, after blocking the light-sensitive channels the contractions were enhanced, more sensitive to light, and saturated at lower intensities, corresponding to only ~1 to 5 effectively absorbed photons per microvillus (Fig. 1, H and I). In the absence of $Ca^{2+}$ influx, such intensities deplete virtually all microvillar $PIP_2$, resulting in temporary loss of sensitivity to light (*10*). After such saturating flashes, the photomechanical response was also temporarily refractory, recovering sensitivity with a time course ($t_{1/2}$ ~ 40 s) similar to that of $PIP_2$ resynthesis (*10*). By contrast, without channel blockers, sensitivity recovered within ~10 s (fig. S3).

Blockade of all light-sensitive current in these experiments also shows that the contractions cannot result from any downstream effects of $Ca^{2+}$ influx or osmotic changes caused by ion fluxes associated with the light response. Therefore, these results indicate that the contractions result from hydrolysis of $PIP_2$. Although we do not exclude other downstream effects of PLC, the speed of the contractions supports a simple and direct mechanism. Cleavage of the bulky head groups from $PIP_2$ molecules, which represent 1 to 2% of lipids in the plasma membrane, leaves DAG in the membrane, which occupies a substantially smaller area than $PIP_2$. This should increase membrane tension, leading to shrinkage of the microvillar diameter, as reported for the action of PLC on the diameter of artificial liposomes (*11*). Integrated over the stack of ~30,000 microvilli, such a mechanism seems capable of accounting for the observed macroscopic contractions, which represent at most ~0.5% of the rhabdomere length (see supplementary text). Within each microvillus, we suggest that the alteration to the mechanical properties of the lipid bilayer may contribute to channel gating.

To test whether phototransduction generates sufficient mechanical forces to gate mechanosensitive channels (MSCs), we made whole-cell patch-clamp recordings from dissociated photoreceptors lacking all light-sensitive channels (*trpl*;*trp* double mutants, or *trpl* mutants exposed to $La^{3+}$ and RR). We then perfused the photoreceptors with gramicidin, a monovalent ($Ca^{2+}$-impermeable) cation channel and one of the best-characterized MSCs, which is known to be regulated by changes in bilayer physical properties (*12*, *13*). Incorporation of gramicidin channels into the membrane generated a constitutive inward current that stabilized after a few minutes (Fig. 2A). Despite having replaced the native light-sensitive channels with MSCs, the photoreceptors still responded to light, with a rapid increase in the gramicidin-mediated current (Fig. 2, B and C). Like the photomechanical responses recorded after blocking $Ca^{2+}$ influx through the light-sensitive channels (Fig. 1H), these gramicidin-mediated responses inactivated slowly (Fig. 2C), were temporarily refractory to further stimulation and had a similar intensity dependence (Fig. 2D).

To test whether the light-sensitive channels were mechanically sensitive, we manipulated membrane tension osmotically. Channels were not directly activated by perfusing cells with hyper- or hypo-osmotic solutions; however, we reasoned

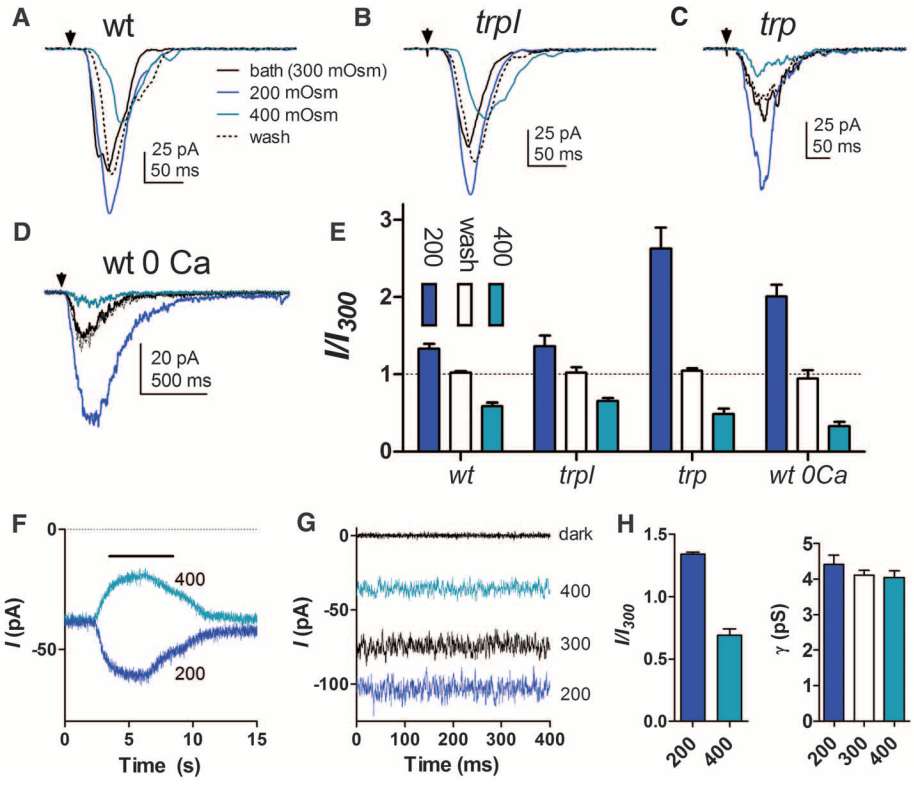


**Fig. 3.** Modulation of light-sensitive channels by osmotic pressure. (**A** to **D**) Whole-cell voltage-clamped responses to 1-ms flashes (~50 effective photons) in control bath (300 mOsm) were reversibly increased by perfusion with 200 mOsm solution and suppressed by 400 mOsm in wild-type (A), *trpl* (B), and *trp* (C) mutants as well as in wild-type photoreceptors recorded in $Ca^{2+}$-free solutions (D). (**E**) Response amplitudes ($I/I_{300}$) after hyperosmotic (400 mOsm) and hypo-osmotic (200 mOsm) challenges normalized to control responses in 300 mOsm bath. Data are means ± SEM; $N$ = 4 to 8 cells. All conditions plotted were significantly increased (200 mOsm) or decreased (400 mOsm) relative to control responses from the same cells [$P$ < 0.005; analysis of variance (ANOVA) followed by posttest for trend]. (**F**) Spontaneous TRP channel activity (from *trpl* mutant) after several minutes of recording, using pipettes lacking nucleotide additives. Perfusion with 400 or 200 mOsm (bar) reversibly suppressed and facilitated this "rundown current" (RDC). (**G**) Channel noise resolved on a faster time base, plus trace recorded in dark before onset of RDC. (**H**) Left: Amplitude of steady-state RDC normalized to value at 300 mOsm. Right: Effective single-channel conductance (γ) estimated by variance/mean ratio (means ± SEM, $N$ = 7). Although macroscopic RDC was substantially modulated ($P$ < 0.001; ANOVA, posttest for trend), single-channel conductance was not significantly affected by osmotic manipulation ($P$ > 0.2).

Downloaded from www.sciencemag.org on March 3, 2013

that it would be impossible to mimic the exact physical effects of $PIP_2$ hydrolysis, which would include a specific combination of changes in membrane tension, curvature, thickness, lateral pressure profile, charge, and pH. We therefore tested whether osmotic manipulation could enhance or suppress light-sensitive channel activity. In wild-type photoreceptors, light-induced currents were rapidly and reversibly facilitated by ~50% after perfusion with hypo-osmotic solutions (200 mOsm), which, like $PIP_2$ depletion, would be expected to alleviate crowding between phospholipids, increase tension, and reduce membrane thickness. Conversely, responses in hyperosmotic (400 mOsm) solutions were about half those in control solutions (Fig. 3). Analysis of single-photon responses (quantum bumps) indicated that modulation resulted from changes in both quantum efficiency (fraction of rhodopsin photoisomerizations generating a quantum bump) and bump amplitude (fig. S4 and supplementary text). Recordings from *trp* and *trpl* mutants showed that both TRP and TRPL channels were modulated, although facilitation of currents mediated by TRPL channels (in *trp* mutants) was more pronounced (Fig. 3). Modulation of the light response by osmotic manipulation was at least as pronounced in $Ca^{2+}$-free bath (Fig. 3D), indicating that facilitation by membrane stretch did not result from leakage of $Ca^{2+}$ into the cell from the extracellular space.

To test whether modulation might have been mediated by effects on upstream components of the cascade such as PLC (*14*), we measured the activity of spontaneously active TRP channels in recordings made with pipettes lacking adenosine triphosphate. Under these conditions, $PIP_2$ becomes depleted (thereby removing PLC's substrate), sensitivity to light is lost, and the TRP channels enter a constitutively active ("rundown") state uncoupled from the phototransduction cascade (*15*, *16*). Nonetheless, the channels were still similarly modulated by osmotic manipulation, whereas single-channel conductance, estimated by noise analysis, was unaffected (Fig. 3, F to H). These results indicate that osmotic pressure directly modulated the open probability of both TRP and TRPL channels.

MSCs such as gramicidin are sensitive to amphiphilic compounds, which insert into the lipid bilayer. Because they are attracted to anionic phospholipids, cationic amphipaths insert preferentially into the inner leaflet, where they increase crowding, promote negative (concave) curvature, and decrease membrane stiffness (*17*, *18*). We found that four structurally unrelated cationic amphipaths were all effective, reversible inhibitors of the light-induced current. Neither light-induced PLC activity (measured using a genetically targeted $PIP_2$-sensitive biosensor to monitor $PIP_2$ hydrolysis) nor single-channel conductance were substantially affected (fig. S5). The 50% inhibitory concentrations ($IC_{50}$ values) were much higher than those of their traditional drug targets and ranged over approximately three orders of magnitude. However, after correcting for $pK_a$ and partitioning, the effective concentration of the compounds in the membrane was similar (~5 mM) in each case (Fig. 4). Thus, their mode of action is likely related to their physicochemical properties rather than conventional drug-receptor interactions. Because cationic amphipaths are also lipophilic weak bases, and because we propose that protons are also critical for activating the light-sensitive channels (*4*), an alternative but not mutually exclusive possible mechanism of action is as lipophilic pH buffers of the membrane environment. We also note that polyunsaturated fatty acids (PUFAs) such as arachidonic and linolenic acid—which are effective activators of both TRP and TRPL (*5*, *19*)—are not only anionic amphipaths (predicted to have opposite effects to cationic amphipaths) but also, as weak acids, natural protonophores; such a dual action could account for their agonist effect.

The mechanism of activation of the light-sensitive channels in invertebrate microvillar photoreceptors has long remained an enigma (*2*, *3*, *20*). Neither $InsP_3$ nor DAG—the two obvious products of $PIP_2$ hydrolysis—are reliable agonists for the light-sensitive channels. Although PUFAs are effective agonists and might be generated from DAG, a DAG lipase with the appropriate specificity has not been found in the photoreceptors (*21*). By contrast, two neglected consequences of PLC activity—the depletion of its substrate ($PIP_2$) together with protons released by $PIP_2$ hydrolysis—were recently shown to potently activate the light-sensitive channels in a combinatorial manner (*4*). Our results support the hypothesis that the effect of $PIP_2$ depletion is mediated mechanically by changes to the physical properties of the lipid bilayer, thereby introducing the concept of mechanical force as an intermediate or "second messenger" in metabotropic signal transduction.

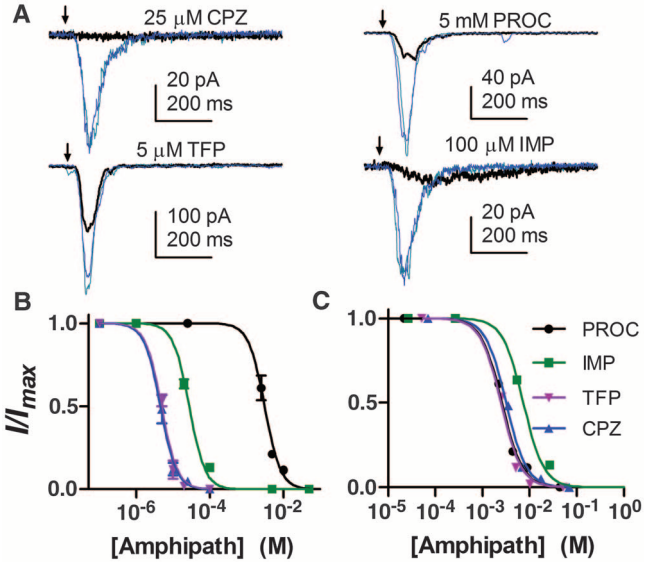


**Fig. 4.** Cationic amphipaths inhibit the light response. (**A**) Response to 1-ms flashes in *trp* mutants in the presence of procaine (PROC), imipramine (IMP), trifluoperazine (TFP), and chlorpromazine (CPZ). Control responses before (turquoise) and after washout (blue) are superimposed. (**B**) Dose response functions (means ± SEM: PROC, $N = 4$; IMP, $N = 3$; TFP, $N = 3$; CPZ, $N = 6$) fitted by inverse Hill curves (slope constrained at $n = 2$), based on raw values ($IC_{50}$: PROC, 3.1 mM; IMP, 27 μM; TFP, 4.9 μM; CPZ, 4.5 μM). (**C**) Same as in (B) after correction for $pK_a$ and octanol partition coefficients, reflecting predicted concentration in the lipid membrane ($IC_{50}$: PROC, 2.7 mM; IMP, 7 mM; TFP, 3.4 mM; CPZ, 2.3 mM).

## References and Notes


1. B. Katz, B. Minke, *Front. Cell. Neurosci.* **3**, 2 (2009).
2. R. C. Hardie, *WIREs Membr. Transp. Signal.* 10.1002/wmts.20 (2012).
3. C. Montell, *Trends Neurosci.* **35**, 356 (2012).
4. J. Huang *et al.*, *Curr. Biol.* **20**, 189 (2010).
5. M. Parnas *et al.*, *J. Neurosci.* **29**, 2371 (2009).
6. A. Patel *et al.*, *Pflugers Arch.* **460**, 571 (2010).
7. S. F. Pedersen, B. Nilius, *Methods Enzymol.* **428**, 183 (2007).
8. K. Franze, *Curr. Opin. Genet. Dev.* **21**, 530 (2011).
9. R. C. Hardie, Y. Gu, F. Martin, S. T. Sweeney, P. Raghu, *J. Biol. Chem.* **279**, 47773 (2004).
10. R. C. Hardie *et al.*, *Neuron* **30**, 149 (2001).
11. J. M. Holopainen, M. I. Angelova, T. Söderlund, P. K. Kinnunen, *Biophys. J.* **83**, 932 (2002).
12. J. A. Lundbaek, S. A. Collingwood, H. I. Ingólfsson, R. Kapoor, O. S. Andersen, *J. R. Soc. Interface* **7**, 373 (2010).
13. O. S. Andersen, R. E. Koeppe 2nd, *Annu. Rev. Biophys. Biomol. Struct.* **36**, 107 (2007).
14. H. Ahyayauch, A. V. Villar, A. Alonso, F. M. Goñi, *Biochemistry* **44**, 11592 (2005).
15. K. Agam *et al.*, *J. Neurosci.* **20**, 5748 (2000).
16. R. C. Hardie, B. Minke, *J. Gen. Physiol.* **103**, 389 (1994).
17. J. A. Lundbaek, *J. Gen. Physiol.* **131**, 421 (2008).
18. B. Martinac, J. Adler, C. Kung, *Nature* **348**, 261 (1990).
19. S. Chyb, P. Raghu, R. C. Hardie, *Nature* **397**, 255 (1999).
20. S. Lev, B. Katz, V. Tzarfaty, B. Minke, *J. Biol. Chem.* **287**, 1436 (2012).
21. H. T. Leung *et al.*, *Neuron* **58**, 884 (2008).


**Acknowledgments:** We thank D. G. Stavenga, S. B. Laughlin, and M. Postma for comments on the manuscript; O. Andersen for advice on the use of gramicidin; and J. Grosche (Effigos AG) for artwork for Fig. 1A. Supported by UK Biotechnology and Biological Sciences Research Council grant BB/G0068651 (R.C.H.) and a UK Medical Research Council Career Development Award (K.F.). Author contributions: project initiation, R.C.H.; whole-cell electrophysiology experiments, R.C.H.; AFM measurements, K.F., R.C.H.; paper written by R.C.H. with contribution from K.F.

## Supplementary Materials

www.sciencemag.org/cgi/content/full/338/6104/260/DC1
Materials and Methods
Supplementary Text
Figs. S1 to S5
Movie S1
References (*22*–*31*)

26 March 2012; accepted 7 August 2012
10.1126/science.1222376

Downloaded from www.sciencemag.org on March 3, 2013